A Journal of the Gesellschaft Deutscher Chemiker

Angewandte International Edition GDCh Chemie

www.angewandte.org

Accepted Article

Title: A Chiral Halogen Bonding [3]Rotaxane for Recognition and Sensing of Biologically-relevant Dicarboxylate Anions

Authors: Jason Y. C. Lim, Igor Marques, Vítor Félix, and Paul D. Beer

To be cited as: *Angew. Chem. Int. Ed.* 10.1002/anie.201711176
Angew. Chem. 10.1002/ange.201711176

Link to VoR: http://dx.doi.org/10.1002/anie.201711176
http://dx.doi.org/10.1002/ange.201711176

WILEY-VCH

10.1002/anie.201711176

WILEY-VCH

A Chiral Halogen Bonding [3]Rotaxane for Recognition and Sensing of Biologically-relevant Dicarboxylate Anions

Jason Y. C. Lim,[a] Igor Marques,[b] Vítor Félix[b] and Paul D. Beer*[a]

Abstract: The unprecedented application of a chiral halogen bonding [3]rotaxane host system for discrimination of stereo- and *E*/*Z* geometric dicarboxylate anion guest isomers is described. Synthesised by a chloride anion templation strategy, the [3]rotaxane host recognises dicarboxylates via formation of 1:1 stoichiometric sandwich complexes, which is supported by molecular dynamics simulations that reveal the critical synergy of halogen and hydrogen bonding interactions in anion discrimination. In addition, the centrally located chiral (*S*)-BINOL motif of the [3]rotaxane's axle component facilitates the complexed dicarboxylate species to be sensed via a fluorescence response.

Dicarboxylates (DC^{2-}) constitute a large and structurally diverse class of anions which play crucial roles in biology and industry,[1] with some (e.g. oxalate) implicated as environmental pollutants.[2] Their biological importance has primarily driven the design and development of polytopic abiotic receptors which utilise hydrogen bonding (HB) interactions[3–12] and Lewis acidic metal centres[13,14] for binding and sensing.[15] However, DC^{2-} are highly challenging targets for selective recognition due to their hydrophilicity[16] and complex overall shapes owing to the diversity of spacer motifs between their anionic carboxylate termini. These linker units can contain one or several chiral centres (e.g. glutamate, tartrate), different functional groups (e.g. C=O, -OH, $-NH_2$) and exhibit geometric isomerism (e.g. *E*/*Z*-alkenes). To further complicate receptor design, these subtle structural differences lead to very similar physicochemical properties amongst isomers. The contrasting bioactivities exhibited by closely-related analogues such as fumarate (*E*-alkene) and maleate (*Z*-alkene)[17–19] provides a powerful impetus to develop abiotic receptors able to recognise and sense dicarboxylates regio-[20–22] and stereoselectively.[23–26]

Mechanically-interlocked molecules such as rotaxanes and catenanes have been exploited for the binding and sensing of charged species.[27–29] Although rare, higher order interlocked host architectures can also provide unique opportunities for host-guest recognition.[30–32] In recent years, halogen bonding (XB), the attractive supramolecular interaction between an electron-deficient halogen atom and a Lewis base, was shown to be highly effective for the recognition of anions, often outperforming HB receptor analogues attributable to XB's more stringent linearity and greater covalent character.[33–37] Herein, we report in a proof-of-concept study, the first example of a chiral XB [3]rotaxane as a novel dicarboxylate receptor (Fig. 1). A chiral (*S*)-1,1'-bi-2-naphthol (BINOL) fluorophore[38] incorporated between two XB-donor 3,5-bis-iodotriazole pyridinium motifs on the axle component, together with two mechanically bonded HB macrocycles, enables the XB [3]rotaxane host to discriminate between DC^{2-} enantiomers (*R* vs *S*-*N*Boc-Glu^{2-}) and geometric isomers (Mal^{2-} vs Fum^{2-}), via fluorescence responses. Chiral discrimination by interlocked host molecules is extremely rare,[39–41] and to the best of our knowledge, an XB [3]rotaxane capable of both geometric and stereoisomer discrimination is unprecedented.

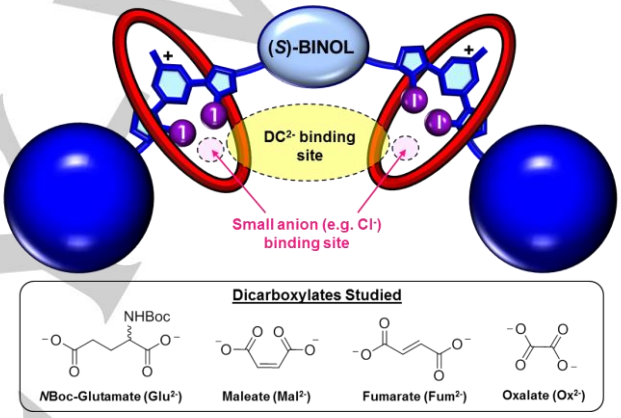

Figure 1. Design of [3]rotaxane host and the structures of the dicarboxylate anions investigated in this study.

The target [3]rotaxane was prepared by a chloride anion-template clipping methodology, exploiting the potent halide affinity of the two 3,5-bis-iodotriazole pyridinium axle motifs, in 37% yield (Scheme 1).[35,42] Electrospray ionisation mass spectrometry (*m*/*z* = 1921 [M^{2+}]) and ^{1}H NMR spectroscopy confirmed the identity and interlocked nature of the [3]rotaxane, which showed dramatic upfield shifts and desymmetrisation of the macrocycle hydroquinone signals (Fig. S2-6). This is consistent with strong donor-acceptor aromatic π-π stacking interactions between the macrocycles and the axle's XB pyridinium units, supported by 2D ROESY spectroscopy (Fig. S2-4), forming the DC^{2-} binding pocket shown in Figure 1.

[a] J.Y.C. Lim, Prof. P.D.Beer
Chemistry Research Laboratory, Department of Chemistry
University of Oxford
12 Mansfield Road, Oxford, OX1 3TA (UK)
E-mail: paul.beer@chem.ox.ac.uk
[b] I. Marques, Prof. V. Félix
Department of Chemistry, CICECO - Aveiro Institute of Materials, and Department of Medical Sciences, iBiMED - Institute of Biomedicine
University of Aveiro
3810-193 Aveiro, Portugal

Supporting information (SI) for this article is given via a link at the end of the document.

10.1002/anie.201711176

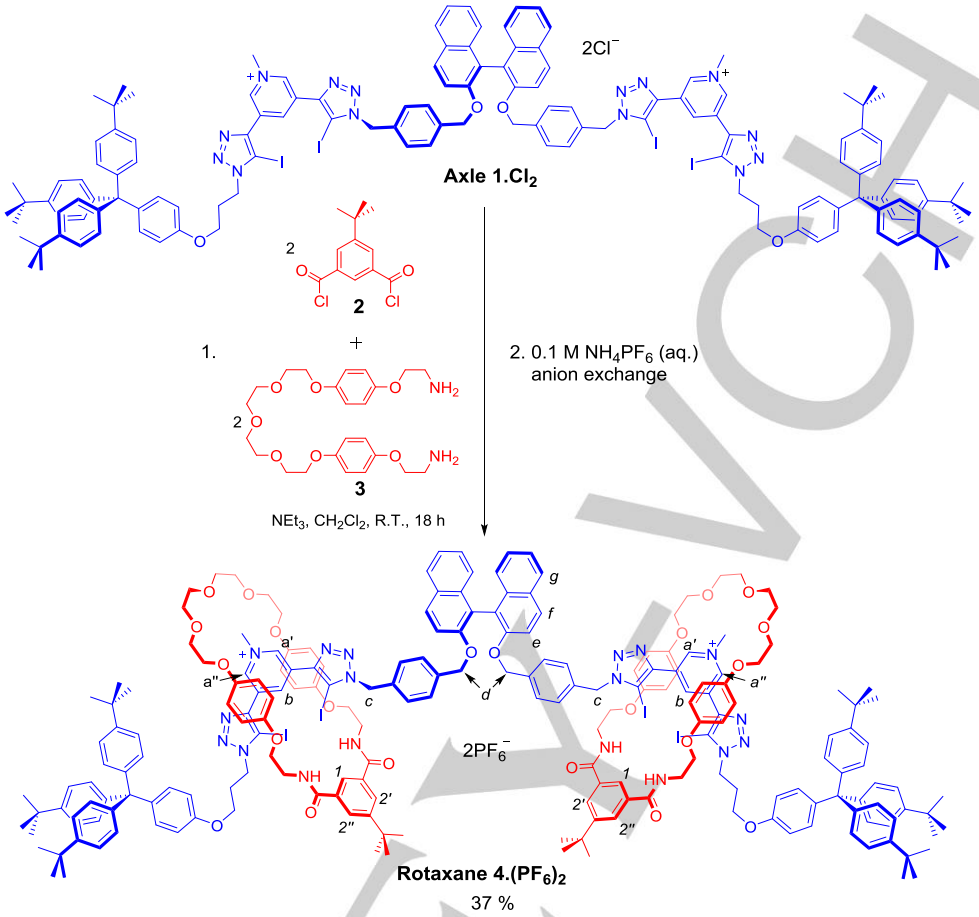

Scheme 1. Chloride anion templated synthesis of [3]rotaxane **4.(PF$_6$)$_2$**.

The anion binding properties of [3]rotaxane **4.(PF$_6$)$_2$** were initially probed using ^{1}H NMR titrations with tetrabutylammonium (TBA) salts of DC^{2-} in $CDCl_3/CD_3OD/D_2O$ 60:39:1 (*v/v*),[43] revealing important differences between DC^{2-} and Cl$^-$ complexation. For example, *S*-Glu^{2-} binding (Fig. 2) is accompanied by modest shifts of signals H_b and H_1, which are much smaller in magnitude in comparison to Cl$^-$ (Fig. S3-1). This suggested that, unlike Cl$^-$, the dianion was too large to fit into each interlocked binding site. *S*-Glu^{2-} binding also elicited greater downfield shifts of axle external pyridinium $H_{a'}$ proton signals than the other ($H_{a''}$), implying a closer proximity to the bound guest. In contrast, Cl$^-$ resulted in similar $H_{a'}$ and $H_{a''}$ signal downfield perturbations without the diagnostic signal 'crossover' seen for *S*-Glu^{2-}. Furthermore, the modest upfield shifts of the centrally-located H_d methylene protons during the *S*-Glu^{2-} titration were absent with Cl$^-$. Together, this ^{1}H NMR titration evidence implied that *S*-Glu^{2-} was binding in the space between both macrocycles to form a 1:1 stoichiometric sandwich complex, whilst Cl$^-$ was likely binding near each individual interlocked cavity. Similar patterns of ^{1}H NMR signal shifts as *S*-Glu^{2-} were seen for *R*-Glu^{2-}, Fum^{2-} and Mal^{2-}, albeit of different magnitudes, clearly indicating that these DC^{2-} guests were binding in the same manner (Fig. S3-2). Circular dichroism spectroscopy of **4.(PF$_6$)$_2$** also revealed much larger spectral changes during Fum^{2-} binding than Cl$^-$ (Fig. S5-1), which suggests larger rotaxane conformational changes occur upon DC^{2-} sandwich complex formation. Although the magnitudes of the respective DC^{2-} anion-induced ^{1}H NMR signal shifts were too small for accurate association constant (*K*) determination using the WinEQNMR2 software,[44] analysis of the H_b shifts with Cl$^-$ using a host-guest 1:2 stoichiometric binding model confirmed the halide's ability to bind strongly within each individual interlocked cavity site ($K_{1:1}$ = 2609 ± 201 M^{-1} and $K_{1:2}$ = 123 ± 10 M^{-1}).

DC^{2-} binding by **4.(PF$_6$)$_2$** was also probed by fluorescence anion titration experiments in $CHCl_3/CH_3OH/H_2O$ 60:39:1 *v/v*, resulting in notable (*S*)-BINOL fluorescence quenching (Fig. 3 and Section S4). In contrast, Cl$^-$ and Ox^{2-} addition elicited much smaller changes, presumably due to their inability to form sandwich complexes. BindFit[45] analysis of the DC^{2-} fluorescence titration data with [3]rotaxane **4.(PF$_6$)$_2$** and free axle **1.(PF$_6$)$_2$** determined the association constants shown in Table 1. For **4.(PF$_6$)$_2$**, the values of $K_{1:1}$ >> $K_{1:2}$ for all DC^{2-} confirmed the 1:1 stoichiometric sandwich complex as the predominant host-guest species. Importantly, **4.(PF$_6$)$_2$** showed impressive chiral discrimination towards *S*-Glu^{2-} with a selectivity of K_S/K_R = 5.7 ± 0.3. **4.(PF$_6$)$_2$** also exhibited a high degree of geometric isomer

discrimination with a selectivity for Fum^{2-} over Mal^{2-} of 4.4 ± 0.3. The importance of the [3]rotaxane structure in DC^{2-} isomer discrimination can be further discerned by comparing its binding behaviour with free axle **1.(PF$_6$)$_2$**. Although the axle alone still displayed appreciable DC^{2-} binding affinities (Table 1), **1.(PF$_6$)$_2$** showed much poorer enantioselectivity (K_S/K_R = 0.96 ± 0.02) for *S*/*R*-Glu^{2-} and complex binding equilibria for Mal^{2-}.[46]

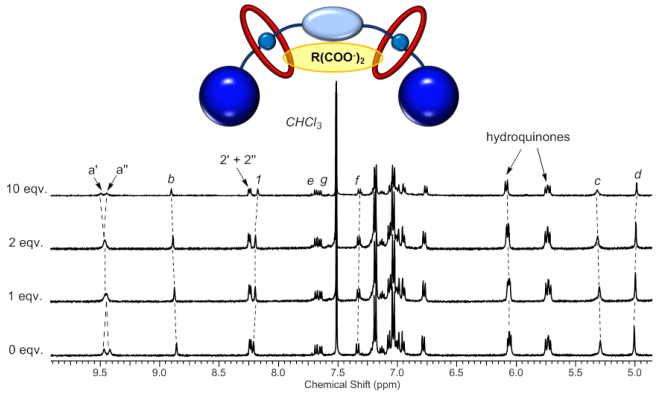

Figure 2. Partial ^{1}H NMR spectra of **4.(PF$_6$)$_2$** in the presence of incremental quantities of *S*-Glu^{2-} ([**4.(PF$_6$)$_2$**] = 1.0 mM, *T* = 298 K, $CDCl_3/CD_3OD/D_2O$ = 60:39:1 *v/v*). Proton labels follow those in Scheme 1.

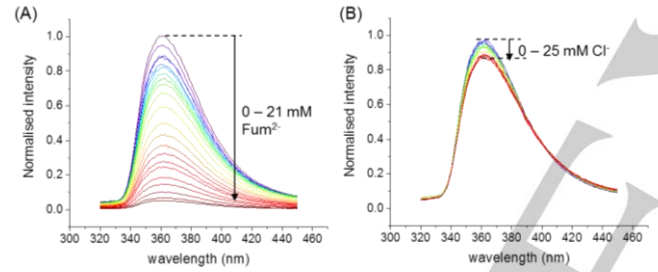

Figure 3. Fluorescence titrations of **4.(PF$_6$)$_2$** with (A) $(TBA)_2(Fum^{2-})$ and (B) TBACl ([**4.(PF$_6$)$_2$**] = 50 μM, λ_{ex} = 280 nm, *T* = 293 K, $CHCl_3/CH_3OH/H_2O$ = 60:39:1 *v/v*).

The origins of the rotaxane's geometric and stereoselective DC^{2-} binding properties were probed with molecular dynamics (MD) simulations using Amber16,[47–49] with the anion complexes immersed in cubic boxes of randomly-distributed solvent molecules in the same ratio used for binding studies. The host and guest molecules were described with GAFF,[50,51] and the XB interactions were simulated with resort to an extra-point of charge (full computational details in Section S6). The 1:1 stoichiometric DC^{2-}-[3]rotaxane complexes (Fig S6-1), were maintained throughout the simulation time via convergent C-I···O_{anion} XB interactions from the axle unit and N-H···O_{anion} hydrogen bonds from the macrocycle components' isophthalamide units (Fig. 4, Tables S6-1 and S6-2).

Table 1. Association constants *K*/ M^{-1} of axle **1.(PF$_6$)$_2$** and rotaxane **4.(PF$_6$)$_2$** with different anions from fluorescence binding studies.[a]

Anion	Rotaxane **4.(PF$_6$)$_2$**	Free axle **1.(PF$_6$)$_2$**
S-Glu^{2-}	$K_{1:1}$ = 35227 ± 2114 $K_{1:2}$ = 13 ± 1	$K_{1:1}$ = 1598 ± 18
R-Glu^{2-}	$K_{1:1}$ = 6226 ± 68 $K_{1:2}$ = 111 ± 1	$K_{1:1}$ = 1660 ± 25
Fum^{2-}	$K_{1:1}$ = 18365 ± 1164 $K_{1:2}$ = 139 ± 1	$K_{1:1}$ = 106 ± 2 K_{12} = 589 ± 9
Mal^{2-}	$K_{1:1}$ = 4179 ± 81 $K_{1:2}$ = 12.6 ± 0.4	-[c]
Ox^{2-}	-[b]	$K_{1:1}$ = 1427 ± 26 $K_{1:2}$ = 357 ± 6

[a] *K* values determined using BindFit[45] to a host-guest 1:2 binding model; *T* = 293 K, [host] = 50 μM, λ_{ex} = 280 nm, $CHCl_3/CH_3OH/H_2O$ 60:39:1 *v/v*; [b] Fluorescence changes too small for *K* value determination; [c] Complex binding equilibria.

[3]Rotaxane discrimination of Mal^{2-} and Fum^{2-} resulted from host-guest size complementarity and differing DC^{2-} solvation within the binding pocket. MP2/6-31+G(d) geometry optimisations revealed the planarity of Fum^{2-}, with an intramolecular carboxylate ($C_{C=O}\cdots C_{C=O}$) distance of 3.987 Å and a dipole moment of 0.00 D, while both carboxylate groups of Mal^{2-} have a relative twist of 47.7° and a 3.440 Å $C_{C=O}\cdots C_{C=O}$ separation, resulting in a 5.20 D dipole moment (Fig S6-2). To accommodate these differing stereoelectronic requirements, the rotaxane underwent a greater structural deformation to bind the latter anion (Fig. 4A), resulting in a decrease of the average distance between the centres of mass of both iodine atoms in each pyridinium bis-iodotriazole motif from 10.48 ± 0.20 Å in free uncomplexed **4.(PF$_6$)$_2$**, to 8.60 ± 0.12 Å and 9.67 ± 0.13 Å for the Mal^{2-} and Fum^{2-} adducts respectively. More importantly, the bound anions are solvated to different extents by H_2O and CH_3OH (Table S6-3). Although CH_3OH is present in a 17-fold molar excess, Mal^{2-}'s carboxylate groups are preferentially solvated by H_2O, while those of the more lipophilic Fum^{2-} are surrounded by more CH_3OH molecules (Table S6-5), following the MD-simulated solvation trends of the free anions as their TBA salts (Table S6-4). Thus, the H_2O molecules strongly compete with the isophthalamide binding unit for the carboxylate groups, leading to 2.9 ± 0.7 $NH_{host}\cdots O_{anion}$ HB interactions for Fum^{2-} and 1.9 ± 0.8 for Mal^{2-} (Table S6-2). Given the comparable XB interactions with both anions (Table S6-1), differing anion solvation mainly accounts for the geometric selectivity of the rotaxane for Fum^{2-}.

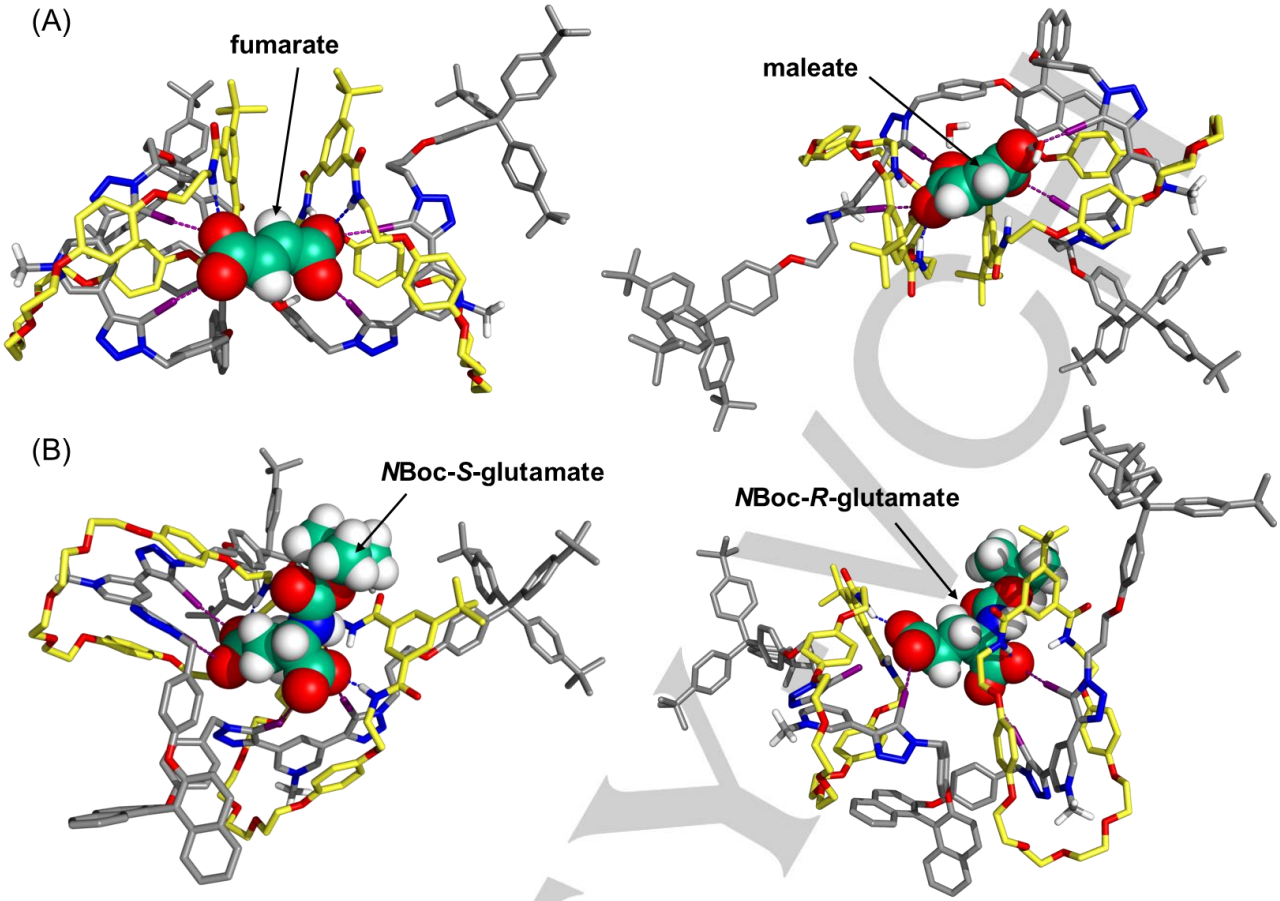

Figure 4. MD illustrative binding scenarios of the 1:1 sandwich complexes of $\mathbf{4}^{2+}$ and (A) Fum^{2-}/Mal^{2-} and (B) *S*/*R*-Glu^{2-}. The XB and HB interactions are depicted as purple and blue dashed lines, respectively.

Contrastingly, the enantioselectivity of $\mathbf{4}^{2+}$ arises primarily from host-guest structural complementarity with less solvent influence. The encapsulated *S*/*R*-Glu^{2-} stereoisomers interact almost exclusively with CH_3OH (Table S6-5), averaging 3.1 ± 0.9 and 1.8 ± 0.7 HB interactions for the *S*- and *R*-enantiomers respectively, which do not significantly interfere with anion binding due to their weakness. However, both anion enantiomers form structurally distinct diastereomeric host-guest complexes (Fig. 4B) with important variations in the extents of their XB and HB interactions. For instance, both carboxylate groups of *R*-Glu^{2-} are held by XB interactions of comparable strengths, while one is more tightly halogen bonded than the other in the *S*-Glu^{2-} complex (Table S6-1). Furthermore, *R*-Glu^{2-} is held by fewer HB interactions (2.8 ± 0.8) than the *S*-enantiomer (3.3 ± 0.9) (Table S6-2). The difference in interaction energy of both diastereomeric complexes (ΔE_{int}) was estimated from the computed molecular mechanics energies of the host-guest complex ($E_{complex}$), free $\mathbf{4}^{2+}$ (E_{host}) and anion (E_{guest}), considering only the electrostatic and van der Waals (vdW) energetic contributions (Table S6-6). Using the equation $\Delta E_{int} = E_{complex} - E_{host} - E_{guest}$, the binding of *S*-$Glu^{2-}$ was favoured over the *R*-enantiomer by *c.a.* 27 kcal mol^{-1}, corroborating the experimental enantioselectivity trend (Table 1).

The MD simulations of axle $\mathbf{1}^{2+}$ with the *S*/*R*-Glu^{2-} show that the absence of the macrocycle units renders XB the only DC^{2-}-binding interaction. At the same time, this increases the exposure of the bound dianion to solvent molecules (Table S6-7), allowing as many as 7 HB interactions to be established between the carboxylate groups and CH_3OH (Table S6-8). Compared to the [3]rotaxane, whose structure is rigidified and preorganised by the presence of both macrocycles, the free axle adopts a more conformationally-flexible DC^{2-} binding cavity. As a result, the binding geometries of the diastereomeric complexes between axle $\mathbf{1}^{2+}$ and *S*/*R*-Glu^{2-} are very similar, such that the anion enantiomers are held together by equivalent numbers of XB interactions (*R*-Glu^{2-}: 3.3 ± 0.7; *S*-Glu^{2-}: 3.0 ± 0.8) (Table S6-9 and Fig S6-3) to give comparable binding affinities. This further highlights the importance of XB/HB synergy and the role of the macrocycle units in governing the augmented selectivity of [3]rotaxane $\mathbf{4.(PF_6)_2}$.

In conclusion, we have reported the first example of a chiral XB [3]rotaxane able to distinguish DC^{2-} enantiomers and geometric isomers via formation of distinct 1:1 stoichiometric sandwich binding complexes. Crucially, smaller anions (e.g. Cl^-) unable to span the length between both macrocycle motifs are bound more weakly and exhibit significantly diminished fluorescence responses compared to DC^{2-} complexation. MD

simulations revealed that the empirical stereo- and geometric DC^{2-} selectivity trends observed for [3]rotaxane **4.$(PF_6)_2$** stem from host-guest complementarity, cooperative synergistic anion coordination by both XB and HB interactions from the rotaxane's framework, as well as important anion-solvent interactions. This proof-of-concept demonstration of higher-ordered interlocked host molecules as highly discriminating sensors for common biologically-relevant DC^{2-} species will stimulate further exploitation of this new class of abiotic mechanically bonded receptors for analytical sensory and nanotechnological applications.

Acknowledgements

J.Y.C. Lim thanks the Agency for Science, Technology and Research (A*STAR), Singapore, for postgraduate funding. The theoretical studies were supported by projects P2020-PTDC/QEQ-SUP/4283/2014, CICECO – Aveiro Institute of Materials (UID/CTM/50011/2013) and iBiMED – Institute of Biomedicine (UID/BIM/04501/2013), financed by National Funds through the FCT/MEC and co-financed by QREN-FEDER through COMPETE under the PT2020 Partnership Agreement. I.M. acknowledges the FCT for PhD scholarship SFRH/BD/87520/2012.

Keywords: dicarboxylates • halogen bonding • molecular recognition • rotaxane • molecular dynamics

[1] D. Voet, J. G. Voet, *Biochemistry*, Wiley, New York, **1995**.
[2] H. Kwon, W. Jiang, E. T. Kool, *Chem Sci* **2015**, *6*, 2575–2583.
[3] H. Fenniri, J.-M. Lehn, A. Marquis-Rigault, *Angew. Chem. Int. Ed. Engl.* **1996**, *35*, 337–339.
[4] R. Gotor, A. M. Costero, P. Gaviña, S. Gil, M. Parra, *Eur. J. Org. Chem.* **2013**, *2013*, 1515–1520.
[5] S.-Y. Liu, L. Fang, Y.-B. He, W.-H. Chan, K.-T. Yeung, Y.-K. Cheng, R.-H. Yang, *Org. Lett.* **2005**, *7*, 5825–5828.
[6] D. Ranganathan, *Acc. Chem. Res.* **2001**, *34*, 919–930.
[7] M. Belen Jimenez, V. Alcazar, R. Pelaez, F. Sanz, A. L. Fuentes de Arriba, M. C. Caballero, *Org Biomol Chem* **2012**, *10*, 1181–1185.
[8] T. Gunnlaugsson, A. P. Davis, J. E. O'Brien, M. Glynn, *Org. Lett.* **2002**, *4*, 2449–2452.
[9] B. R. Linton, M. S. Goodman, E. Fan, S. A. van Arman, A. D. Hamilton, *J. Org. Chem.* **2001**, *66*, 7313–7319.
[10] J. M. Benito, M. Gómez-García, J. L. Jiménez Blanco, C. Ortiz Mellet, J. M. García Fernández, *J. Org. Chem.* **2001**, *66*, 1366–1372.
[11] S. K. Kim, B.-G. Kang, H. S. Koh, Y. J. Yoon, S. J. Jung, B. Jeong, K.-D. Lee, J. Yoon, *Org. Lett.* **2004**, *6*, 4655–4658.
[12] S. Carvalho, R. Delgado, N. Fonseca, V. Felix, *New J Chem* **2006**, *30*, 247–257.
[13] P. D. Beer, M. G. B. Drew, C. Hazlewood, D. Hesek, J. Hodacova, S. E. Stokes, *J Chem Soc Chem Commun* **1993**, 229–231.
[14] C. V. Esteves, P. Mateus, V. André, N. A. G. Bandeira, M. J. Calhorda, L. P. Ferreira, R. Delgado, *Inorg. Chem.* **2016**, *55*, 7051–7060.
[15] D. Curiel, M. Más-Montoya, G. Sánchez, *Coord. Chem. Rev.* **2015**, *284*, 19–66.
[16] S. E. McLain, A. K. Soper, A. Watts, *J. Phys. Chem. B* **2006**, *110*, 21251–21258.
[17] S. Angielski, J. Rogulski, *Acta Biochim. Pol.* **1962**, *9*, 357–365.
[18] A. Munnich, *Nat Genet* **2008**, *40*, 1148–1149.
[19] S. Eiam-ong, M. Spohn, N. A. Kurtzman, S. Sabatini, *Kidney Int.* **1995**, *48*, 1542–1548.
[20] F. Sancenón, R. Martínez-Máñez, M. A. Miranda, M.-J. Seguí, J. Soto, *Angew. Chem.* **2003**, *115*, 671–674.
[21] Y.-P. Tseng, G.-M. Tu, C.-H. Lin, C.-T. Chang, C.-Y. Lin, Y.-P. Yen, *Org Biomol Chem* **2007**, *5*, 3592–3598.
[22] M. M. Santos, I. Marques, S. Carvalho, C. Moiteiro, V. Felix, *Org Biomol Chem* **2015**, *13*, 3070–3085.
[23] S. Rossi, G. M. Kyne, D. L. Turner, N. J. Wells, J. D. Kilburn, *Angew. Chem. Int. Ed.* **2002**, *41*, 4233–4236.
[24] J. L. Sessler, A. Andrievsky, V. Král, V. Lynch, *J. Am. Chem. Soc.* **1997**, *119*, 9385–9392.
[25] S. Bartoli, T. Mahmood, A. Malik, S. Dixon, J. D. Kilburn, *Org Biomol Chem* **2008**, *6*, 2340–2345.
[26] T. Ikeda, O. Hirata, M. Takeuchi, S. Shinkai, *J. Am. Chem. Soc.* **2006**, *128*, 16008–16009.
[27] M. J. Langton, P. D. Beer, *Acc. Chem. Res.* **2014**, *47*, 1935–1949.
[28] M. Xue, Y. Yang, X. Chi, X. Yan, F. Huang, *Chem. Rev.* **2015**, *115*, 7398–7501.
[29] J. E. M. Lewis, M. Galli, S. M. Goldup, *Chem Commun* **2017**, *53*, 298–312.
[30] Y. Nagawa, J. Suga, K. Hiratani, E. Koyama, M. Kanesato, *Chem Commun* **2005**, 749–751.
[31] M. J. Langton, P. D. Beer, *Chem. – Eur. J.* **2012**, *18*, 14406–14412.
[32] T. A. Barendt, A. Docker, I. Marques, V. Félix, P. D. Beer, *Angew. Chem. Int. Ed.* **2016**, *55*, 11069-11076.
[33] L. C. Gilday, S. W. Robinson, T. A. Barendt, M. J. Langton, B. R. Mullaney, P. D. Beer, *Chem. Rev.* **2015**, *115*, 7118–7195.
[34] G. Cavallo, P. Metrangolo, R. Milani, T. Pilati, A. Priimagi, G. Resnati, G. Terraneo, *Chem. Rev.* **2016**, *116*, 2478–2601.
[35] S. W. Robinson, C. L. Mustoe, N. G. White, A. Brown, A. L. Thompson, P. Kennepohl, P. D. Beer, *J. Am. Chem. Soc.* **2015**, *137*, 499–507.
[36] T. M. Beale, M. G. Chudzinski, M. G. Sarwar, M. S. Taylor, *Chem Soc Rev* **2013**, *42*, 1667–1680.
[37] A. Brown, P. D. Beer, *Chem Commun* **2016**, *52*, 8645–8658.
[38] L. Pu, *Acc. Chem. Res.* **2012**, *45*, 150–163.
[39] N. Kameta, Y. Nagawa, M. Karikomi, K. Hiratani, *Chem Commun* **2006**, 3714–3716.
[40] R. Mitra, M. Thiele, F. Octa-Smolin, M. C. Letzel, J. Niemeyer, *Chem Commun* **2016**, *52*, 5977–5980.
[41] J. Y. C. Lim, I. Marques, V. Félix, P. D. Beer, *J. Am. Chem. Soc.* **2017**, *139*, 12228–12239.
[42] B. Nepal, S. Scheiner, *Chem. – Eur. J.* **2015**, *21*, 13330–13335.
[43] An excess of $CDCl_3$ was necessary to maintain **4.PF_6** solubility during the titration, while wet CD_3OD was essential for good ^{1}H NMR spectral resolution and data fitting to reasonable binding models.
[44] M. J. Hynes, *J. Chem. Soc. Dalton Trans.* **1993**, 311–312.
[45] *www.supramolecular.org*.
[46] While the fluorescence of axle **1.$(PF_6)_2$** was still insensitive to Cl^- binding (Section S4, SI), significant perturbations resulted from oxalate binding, likely due to greater flexibility of the host framework unconstrained by the steric demands of the macrocycle components in **4.$(PF_6)_2$**.
[47] D. A. Case, R. M. Betz, W. Botello-Smith, D. S. Cerutti, I. T.E. Cheatham, T. A. Darden, R. E. Duke, T. J. Giese, H. Gohlke, A. W. Goetz, et al., *AMBER 2016*, University Of California, San Francisco, **2016**.
[48] R. Salomon-Ferrer, A. W. Götz, D. Poole, S. Le Grand, R. C. Walker, *J. Chem. Theory Comput.* **2013**, *9*, 3878–3888.
[49] S. Le Grand, A. W. Götz, R. C. Walker, *Comput. Phys. Commun.* **2013**, *184*, 374–380.
[50] J. Wang, R. M. Wolf, J. W. Caldwell, P. A. Kollman, D. A. Case, *J. Comput. Chem.* **2004**, *25*, 1157–1174.
[51] J. Wang, R. M. Wolf, J. W. Caldwell, P. A. Kollman, D. A. Case, *J. Comput. Chem.* **2005**, *26*, 114–114.

10.1002/anie.201711176

WILEY-VCH

Entry for the Table of Contents (Please choose one layout)

Layout 1:

COMMUNICATION

The first chiral halogen bonding [3]rotaxane capable of discriminating between dicarboxylate stereo- and geometric isomers via fluorescence spectroscopy is reported. Computational modelling studies reveal the critical synergy between the rotaxane host's axle and macrocycle components in achieving dicarboxylate guest selectivity.

*Jason Y. C. Lim, Igor Marques, Vítor Félix and Paul D. Beer**

Page No. – Page No.

A Chiral Halogen Bonding [3]Rotaxane for Recognition and Sensing of Biologically-relevant Dicarboxylate Anions